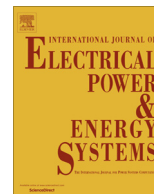




Contents lists available at ScienceDirect

Electrical Power and Energy Systems

journal homepage: www.elsevier.com/locate/ijepes

Assessment of reactive power contribution of photovoltaic energy systems on voltage profile and stability of distribution systems



Mohamed M. Aly^a, Mamdouh Abdel-Akher^{a,c}, Zakaria Ziadi^{b,*}, Tomonobu Senjyu^b

^a Department of Electrical Engineering, Aswan Faculty of Engineering, Aswan University, 81542 Aswan, Egypt

^b Faculty of Engineering, University of the Ryukyus, 1 Senbaru Nishihara-cho, Nakagami, Okinawa 903-0213, Japan

^c Electrical Engineering Department, College of Engineering, Qassim University, King Abdulaziz Road, Unaizah 56434, Qassim, Kingdom of Saudi Arabia

ARTICLE INFO

Article history:

Received 3 September 2012

Received in revised form 14 January 2014

Accepted 18 February 2014

Keywords:

Voltage stability

Regulation

Continuation power-flow

Photovoltaic energy systems

Reactive power

Cloud effects

ABSTRACT

This paper studies the impact of large-scale photovoltaic (PV) generation, up to 50% penetration level, on distribution system voltage regulation and voltage stability. The system voltage profiles are computed using power-flow calculations with load variation of a 24-h time scale. The steady-state voltage stability is examined at different times of the day using a developed continuation power-flow method with demand as continuation parameter and up to the maximum loading conditions. The load-flow analysis, implemented for both voltage regulation and voltage stability analysis, is performed by using the forward/backward sweep method. The secant predictor technique is developed for predicting the node voltages which are then corrected using the load flow solver. Three models of the PV interface inverter are implemented in this study with full set of data representing environmental conditions. The voltage profiles are regulated using the PV interface inverters, where the available inverter capacity is utilized for regulating the system node voltages. The most possible scenarios of system voltage collapse are investigated at different times of the study period. The developed methods and models are used to assess the performance of a 33-bus radial distribution feeder which operates with a high level of PV penetration. The results show that the PV interface inverters operate for reactive power support in distribution system resulting in improved voltage profile, secure power systems operation, and increasing the lifetime of the online tap changing transformers due to minimizing the total number of switching operations.

© 2014 Elsevier Ltd. All rights reserved.

Introduction

Nowadays, renewable energy sources become a more significant source of energy in the new millennium. Among these renewable energy sources, PV energy resources are attracting a growing amount of interest due to the gradual development of technology and the reduction of PV system cost. Besides assisting in the reduction of the emission of greenhouse gases, they add the much-needed flexibility to the energy resource mix by decreasing the dependence on fossil fuels. Therefore, the installed capacity of grid-connected PV power system installations has grown dramatically over the last five years [1]. The PV directly converts sunlight into electricity using the photoelectric effect. The production of electricity from solar sources depends on the amount of light energy in a given location. Solar output varies throughout the day and through the seasons. Grid-connected PV systems are

designed to inject all of the real power produced by PV modules [2]. They are represented as negative power loads. The size of the negative PV load is dependent on the environment conditions, i.e., radiation and temperature. Large-scale PV generation has been considered as an important new alternative energy in the 21st century's energy structure [3].

Furthermore, most of the new PV capacity has been installed in the distribution grid as distributed generation. As PV penetration levels increase, its integration impact on electric networks draws researchers' concern around the world [4,5]. The size of the PV system, its location on the circuit, the impedance of the system, and the way the PV inverter operates, will determine its impact on the system voltage [6]. One of the important issues is to understand the impact of large-scale grid-connected solar PV generations on system voltage [7,8]. As the penetration level of PV generation increases, it will have impact on the voltage stability and regulation of distribution systems. Because its operation depends on environmental conditions, the characteristics of PV systems may be different from those of typical synchronous generators [9].

* Corresponding author. Tel./fax: +81 98 895 8686.

E-mail addresses: mmam72@gmail.com (M.M. Aly), mabdelaakher@ieee.org (M. Abdel-Akher), ziadizaki@yahoo.com, b985542@tec.u-ryukyu.ac.jp (Z. Ziadi).

Voltages at the customer service entrance are maintained by utilities within an acceptable range to ensure adequate operation and lifetime of customer equipment. This is achieved by on-load tap changing transformers (OLTC) and reactive power support [10]. Reactive power supply is also essential for reliable operation of the electric power systems. The shortage of reactive power supply can contribute to voltage collapse, as reported in several recent major power outages [11]. It has been proved that inadequate reactive power compensation during stressed operating condition can lead to voltage instability [12]. Capacitor banks are widely used in power systems for voltage regulation. However, capacitor banks are switched on or off, which are not a continuous variable real-time source of reactive power. Moreover, the reactive power from capacitor banks decreases as the system voltage decreases (by voltage squared) when reactive power is most needed [13].

Without or with small penetration of PV generation, fluctuations in loads and voltage levels in most distribution systems are relatively small and predictable and so the relatively slow operation of OLTCs and VAR devices is acceptable [14]. However, the fluctuations are not predictable when distribution systems are subject to large scale PV generation. In this situation, OLTCs and VAR devices will not be sufficient to ensure adequate voltage regulation because the variability of PV generation can occur on a timescale much shorter than the present equipment can deal with. The output of a PV module can be reduced dramatically when even a small portion of it is shaded by cloud. For instance, cloud transients can cause ramps in PV generation on the order of 15% per second at a particular location slowing to perhaps 15% per minute for an entire distribution circuit due to its spatial diversity [1]. Therefore, for PV generation resources to maintain the voltages within the acceptable limit, they should have the capability of producing reactive power in addition to the active power for voltage support.

A number of publications [13,15,16] are available that address the benefits of using inverter-based distributed generation for voltage support. Several studies have been conducted to examine the possible impacts of high levels of utility penetration of this type of PV system. One of the first issues studied was the impact on power system operation of PV system output fluctuations caused by cloud transients [1]. Cloud transient effects on voltage profile were investigated in large scale transmission level [17]. Due to the special characteristics of distribution networks, performance achieved in a large-scale transmission system does not necessarily mean the same performance in distribution systems. The PV power support may lose most of its power within a short period in distribution systems due to cloud coverage. Cloud transient effects on voltage profile in small scale three-phase distribution system were investigated in [18].

Voltage stability steady-state analyses can be assessed by obtaining voltage profiles of critical buses as a function of their loading conditions. These voltage profiles, or shortly P - V curves, provide considerable insight into the systems behavior and operating conditions for different loading levels, and have been used by the electric power industry for assessing voltage stability margins and the areas prone to voltage collapse [19]. The gradual load increment will lead to a saddle-node bifurcation (SNB) point which corresponds to the maximum loading point (MLP), as shown in Fig. 1 [20,21]. Under these conditions, the Jacobian matrix becomes singular.

In this paper, the steady-state voltage profile and voltage stability of a large scale grid-connected PV power station is discussed under clear sky condition and cloudy sky condition at 50% PV penetration level. Moreover, effects of irradiance and temperature are studied. The PV power station applies a maximum power point tracking (MPPT) strategy where the generated real power of PV system depends mainly on weather conditions. The flow of reactive

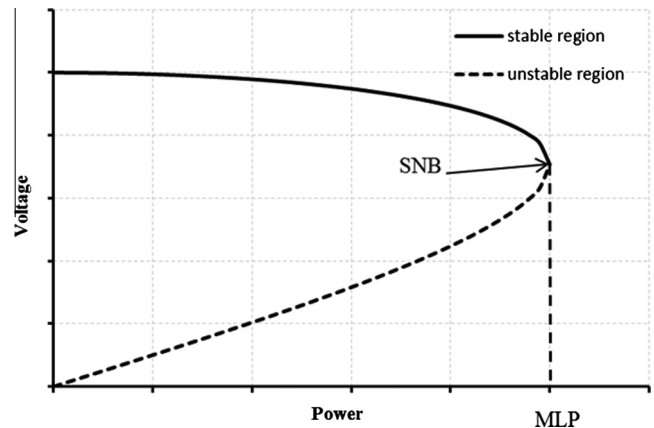


Fig. 1. A typical PV curve.

power in the feeder was investigated with different assumptions of inverter participation. The reactive power is also varying with the weather conditions whereas the constraint is satisfied at all time. Different models of PV inverter were studied together with different cases during the time of the day with clear sky and cloud incidents. These studies were performed on the IEEE 33-bus radial distribution system.

For voltage regulation analysis, the target is to hold all customers within the band of $\pm 5\%$ voltage during the 24 h of the day [22]. The voltage stability analyses are examined at different times of the day by continuation power-flow (CPF) as the load increment up to the MLP. The PV power station was divided between bus 18 and bus 33 as they are the weakest buses in the distribution system under study. Results for voltage regulation and voltage stability were plotted for bus 18 only to avoid repetition. The simulations were done by MATLAB M-file programming.

The organization of this paper is as follows: 'Reactive power support by PV conditioning unit' describes the reactive power support by PV inverter. 'Continuous Power-Flow Analysis' describes the continuous power-flow analysis. 'Modeling of PV array power' describes the modeling of PV array power. 'Results and discussion' analyzes the simulation results and discussions. Finally, 'Conclusion' provides conclusions regarding this work.

Reactive power support by PV conditioning unit

Currently, standards such as IEEE1547 [23] state that the PV inverter shall not actively regulate the voltage at the PCC. Therefore, PV systems are designed to operate at unity power factor (i.e., must not inject or consume reactive power or in any way attempt to regulate voltage). The inverter should be designed for this contribution in the first place in order not to cut into the real power capability of the PV because cutting into the real power capability has negative economic consequences for the owner [6].

To mitigate the above problem, it has been proposed that the interconnection standards for inverter based PV generation be changed in such a way to enable the inverters to assist with high speed voltage regulation [1,4,6]. In this case, the PV inverter will be required to have a maximum apparent power capability larger than the maximum power output of its PV array and the excess capability will be dispatched by the distribution utility for voltage regulation. Inverters with modern digital signal processor-based control systems have the potential to offer an economical, highly flexible means to control both real and reactive power flows under normal operating conditions. These inverters have quicker response and a larger reactive power adjustment range at rated real power than the excitation circuit of the synchronous machines [10].

Modern inverters used for PV are typically pulse-width modulated (PWM) units with switching bridges composed of insulated gate bipolar transistors (IGBT) [6]. In theory, this type of switching technology is able to operate in all four power quadrants, as shown in Fig. 2. Active participation of the PV inverters with system voltage regulation will be helpful to manage system voltage conditions, so inverters will need to provide reactive power control to do this. By adjusting reactive power output, system voltage regulation can be assisted; positive reactive power raises the voltage and negative reactive power lowers the voltage. For active regulation, the inverter will usually operate in quadrants 1 or 2 for grid-connected operation or perhaps even in 3 or 4 if equipped with some form of energy storage for stand-alone operation.

Active system regulation features embedded within inverters will be helpful for high-penetration PV situations to help regulate voltage. A key factor that determines the capability of inverters to assist with system regulation is the number of quadrants in which they operate. Two-quadrant operation (the topic of this paper), as shown in Fig. 3 includes positive real power with lagging VARs or positive real power with leading VARs, and this is fine for many voltage regulation needs of the 21st century power system [6].

The reactive power capabilities of PV inverters can be used to offset the reactive load. This reduces the reactive power flow on the distribution feeder, and in turn reduces the voltage drop along the feeder. Although conventionally the range of the reactive power supply from such devices is limited, it is possible to upgrade the inverters to supply reactive power in a much larger range. Oversizing of the inverter will significantly increase the range of reactive power supply. In all the studied cases, inverters with 10% increased ratings were used, to allow for ample reactive power capability. Implementing this feature would require modifications to the traditional PV inverter hardware design. For example, the required rating of the PV power electronics would have to be suitably oversized to support reactive needs and maintain full real power service [4].

The inverter's ratings are represented by a vector with magnitude S , i.e. the magnitude of the apparent power, the power produced by PV array is P_{pv} , and the reactive power is Q_g . By

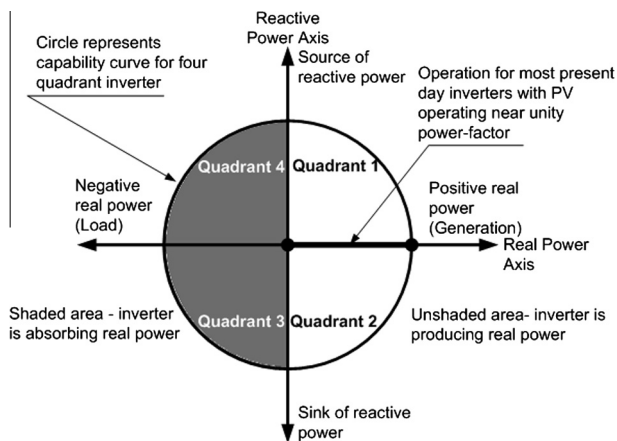


Fig. 2. Quadrants of inverter operation.

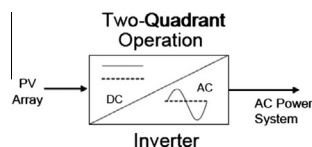


Fig. 3. Inverter devices capable of two-quadrant operation.

increasing the inverter size by 10%, making $S = 1.1P_{pv,max}$, the reactive power capability can be increased from zero to nearly 46% in the maximum PV power generation condition. However, the losses in an inverter are expected to rise as power factor drops because as the inverter's power factor drops, the inverter must source more current. Thus, the inverter switching losses as well as the conduction losses are proportional to the current and its square respectively [24]. Consequently, Modes 2 and 3 of operation may affect the inverter's power conversion efficiency and this is fully exploited in the developed method.

Continuous power-flow analysis

The continuous power-flow is performed for the stable part of the P - V curve up to the MLP. The procedure consists of two steps as follows [25,26]:

The predictor step

The stable part is calculated using the secant predictor technique, the first order (linear) of Lagrangian interpolating polynomial [27], which is widely used in continuation power-flow methods. In this technique, the first two points are calculated using the power-flow analysis method. These two points forms the base for predicting the next points using extrapolating beyond the second point. In this method, the straight line equation of this line connect the two points is used to estimate a third point on the line. This point is a predictor point and is entered as an initial point for the power-flow solution to find the corrected solution. This technique decreases the number of iterations as the predicted point in each step is not far much from the corrected one. The aforementioned is generalized as exhibited in Fig. 4. Suppose a non-linear function $F(x)$, is expressed as follows:

$$Y = F(x) \tag{1}$$

For given two points (x^{k-1}, y^{k-1}) and (x^k, y^k) on the function Y , the straight line equation connected between them is given by:

$$SL = \frac{y^k - y^{k-1}}{x^k - x^{k-1}} = \frac{\Delta y^{k,k-1}}{\Delta x^{k,k-1}} \tag{2}$$

where

- SL refers to the slope of the line.
- k refers to the point serial on the curve.
- x, y are state variables of the function F .

The predicted solution at the point (x^{k+1}, y^{k+1}) is given as follows:

$$SL^{k,k+1} = \frac{y^{k+1,PR} - y^{k,CR}}{x^{k+1} - x^k} = \frac{y^{k+1,PR} - y^{k,CR}}{\Delta x^{k,k+1}} \tag{3}$$

$$y^{k+1,PR} = SL^{k,k+1}(\Delta x^{k,k+1}) + y^{k,CR} \tag{4}$$

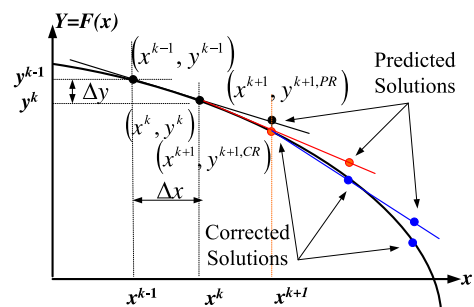


Fig. 4. Secant predictor technique.

where

PR superscript refers to the predicted solution.
CR superscript refers to the corrected solution.

Eqs. (3) and (4) can be written for a power system at bus i as follows:

$$V_i^{k+1,PR} = SL_{V_i}^{k,k+1} (\Delta\lambda^{k,k+1}) + V_i^{k,CR} \quad (5)$$

$$\delta_i^{k+1,PR} = SL_{\delta_i}^{k,k+1} (\Delta\lambda^{k,k+1}) + \delta_i^{k,CR} \quad (6)$$

where

V_i the voltage magnitude at bus i .
 δ_i the angle of the voltage at bus i .
 SL_{V_i} the slope of the predictor of the voltage magnitude at bus i .
 SL_{δ_i} the slope of the predictor of the voltage magnitude at bus i .
 λ the continuation parameter factor.

In this paper, the system demand is considered continuation which is expressed at bus i as follows:

$$P_i^k = (1 + K_{P_i}\lambda)P_{i,0} \quad (7)$$

$$Q_i^k = (1 + K_{Q_i}\lambda)Q_{i,0} \quad (8)$$

where

$P_{i,0}, Q_{i,0}$ the active and reactive powers at the base load, can be considered initially equal to zero.
 P_i^k, Q_i^k the active and reactive powers at point k .
 K_i the load multiplier at bus i .

The corrector step

The corrector step is performed by using the forward/backward substitution method [28,29]. The backward sweep of load currents are performed from downstream to upstream of the system where the bus voltages are performed from upstream to downstream of the system. Consider a radial distribution system having N buses and $B(=N-1)$ branches where the node number 1 is reserved for the source. The forward–backward substitution method is summarized in the following three steps:

Step 1 : Current injection due to loads and capacitor banks and other shunt elements

$$I_i = \left(\frac{P_i + jQ_i}{V_i} \right)^* \quad i = 2, 3, \dots, N. \quad (9)$$

Step 2 : The current summation process towards the source node is referred as the backward sweep. The branch current J of a line segment x connected between buses i and j is calculated as follows:

$$J_x = I_j + \sum_{m \in M} J_m \quad (10)$$

where

J_m the current flows in line section m .
 M is the set of line sections connected downstream to node j .

Step 3 : : The third step in the solution process is the voltage update or the forward sweep step. In this step with the knowledge of the voltage at the substation node and the

branch currents, the downstream nodes are calculated as follows:

$$V_j = V_i - Z_{ij}J_m \quad (11)$$

After computing the above three steps, the power mismatches at each node are calculated as follows:

$$\Delta S_i = S_i^{CL} - S_i^{LD} < \varepsilon \quad (12)$$

where

ΔS_i the complex apparent power mismatch at bus i .
 S_i^{CL} the calculated power at bus i .
 S_i^{LD} the load demand at bus i .
 ε preset tolerance mismatch.

Also, the voltage mismatch can be used to test out the convergence of the power-flow solution as follows:

$$\Delta|V_i| < \varepsilon \quad (13)$$

where

$\Delta|V_i|$ the voltage magnitude difference between two successive iterations.

The step length can be either fixed or adaptive. As the simulation is performed on real time, the step used is of fixed type.

Modeling of PV array power

PV array real power

The basic element of the PV array is the solar cell which usually uses a $p-n$ junction diode in a physical configuration to produce PV electricity. The PV module is the result of associating a group of PV cells in series and parallel and it represents the conversion unit in this generation system. The PV array is an arrangement of several modules connected in series/parallel to get a suitable power and voltage. The electrical power output from a PV panel depends on the incident solar radiation, the cell temperature and the solar incidence angle. The irradiance is the main factor effecting PV array power, so that the system operation status will vary with irradiance change. The real power has a linear increment with irradiance. The equivalent circuit of the PV cell and the equations for current and voltage are cited in the different literature articles [30,31].

There are several approaches to control the power output of PV, and MPPT algorithm is the most common method [32]. The algorithm is used to maintain the voltage of PV panel at a certain point such that the power output is maximized. Power electronic converters are usually required to process the electricity from the PV device. These converters may be used to regulate the voltage and current at the load, to control the power flow in grid-connected systems, and for MPPT of the device.

The possibility of predicting a PV plant's behavior in various irradiance, temperature and load conditions is very important for sizing the PV plant and converter, as well as for the design of the MPPT and control strategy. Manufacturers often provide an indicator called the NOCT, which stands for nominal operating cell temperature. The NOCT is cell temperature in a module when ambient is 20 °C and solar irradiation is 0.8 kW/m² [33]. To account for other ambient conditions, Eq. (14) is used [32].

$$T_{cell} = T_{amb} + (T_{NOCT} - 20) \frac{G}{0.8} \quad (14)$$

where

T_{cell} is cell temperature °C.
 T_{amb} is ambient temperature °C.
 G is solar insolation (kW/m^2).

As cell temperature increases, V_{oc} decreases substantially while I_{sc} increases only slightly. Dependence of V_{oc} on cell temperature is given by Eq. (15) [31].

$$V_{oc} = V_{oc,n}[1 + k_V(T_{cell} - T_n)] \quad (15)$$

where

V_{oc} is the open circuit voltage at T_{cell} .
 $V_{oc,n}$ is the open circuit voltage at standard temperature.
 k_V is the coefficient of decreasing V_{oc} by increasing T_{cell} ($\text{V}/^\circ\text{C}$).
 T_n is the standard temperature (25°C).

As the insolation drops, I_{sc} drops in direct proportion. Decreasing insolation also reduces V_{oc} , but it does so following a logarithmic relationship that results in relatively modest changes in V_{oc} . Dependence of I_{sc} on insolation is given by Eq. (16) [2].

$$I_{sc} = [I_{sc,n} + k_I(T_{cell} - T_n)] \frac{G}{G_n} \quad (16)$$

where

I_{sc} is the short circuit current at G .
 $I_{sc,n}$ is the short circuit current at standard temperature.
 k_I is the coefficient of decreasing I_{sc} by decreasing G ($\text{A}/^\circ\text{C}$).
 G_n is the standard insolation ($1000 \text{ W}/\text{m}^2$).

A quantity that is often used to characterize module performance is the fill factor (FF). The fill factor is the ratio of the power at the maximum power point to the product of V_{oc} and I_{sc} as shown in Eq. (17). Fill factors around 70–75% for crystalline silicon solar modules are typical [31].

$$P_{max} = FF \times V_{oc} \times I_{sc} \quad (17)$$

where

P_{max} is the DC power at the maximum power point tracking.

The conversion efficiency from DC to AC power accounts for inverter efficiency. The AC output power is given in Eq. (18).

$$P_{ac} = \eta_{converter} \times P_{max} \quad (18)$$

where

P_{ac} is the AC power output of the inverter.
 $\eta_{converter}$ is the inverter efficiency.

The shell SM50 – H, a typical 50 W PV module, was chosen for modeling. T_{NOCT} is (45°C) and the key specifications are shown in Table 1 [34]. The clear-sky insolation distributions on 21st of March for a city at Latitude (40°N) are shown in Fig. 5 [32].

Table 1
Data at standard test conditions.

P_{MPPT}	50 W
$I_{sc,n}$	3.4 A
$V_{oc,n}$	19.8 V
k_I	1.4 ($\text{mA}/^\circ\text{N}$)
k_V	-70 ($\text{mV}/^\circ\text{N}$)

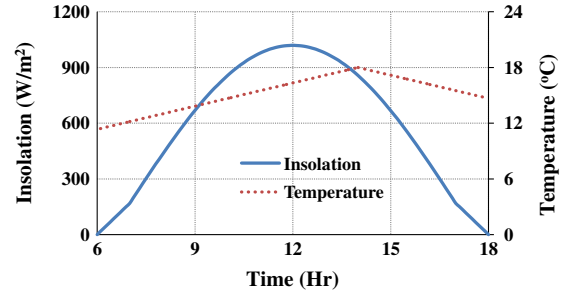


Fig. 5. The insolation and temperature distributions used in the (X-axis: Time (h), Y-axis left: Insolation (W/m^2), Y-axis right: Temperature ($^\circ\text{C}$)).

Reactive power calculation

When inverter with capability beyond the IEEE1547 standard is reviewed and the PV system applies MPPT strategy, the value of Q_g is determined according to Eq. (19) [35].

$$Q_g < \sqrt{S^2 - P_{ac}^2} \quad (19)$$

where

S is the magnitude of the apparent power.
 Q_g is the reactive power generated by the inverter.

Results and discussion

The effect of large-scale PV penetration on the steady state voltage stability and regulation of radial distribution systems has been tested using the 33-node radial feeder. The feeder is shown in Fig. 6 and the complete data of this feeder is found in [36]. This feeder is assumed to include urban residential, commercial, light industrial and street lighting loads. The daily load curves (DLCs) of normalized active and reactive powers demand are shown in Fig. 7(a) and Fig. 7(b) respectively [37]. The data in [36] is assumed equal to approximately the average values in the DLCs which are taken to be equal to 65% of the urban residential load and 50% for the other loads.

Voltage regulation results

Three models were considered at these analyses. Description of these models is as follows:

Model 1: The inverter is assumed to operate at unity power factor (IEEE1517 standard).

Model 2: The inverter is allowed to generate reactive power for voltage support. The S rating of the inverter is assumed equal to $100\%P_{max}$.

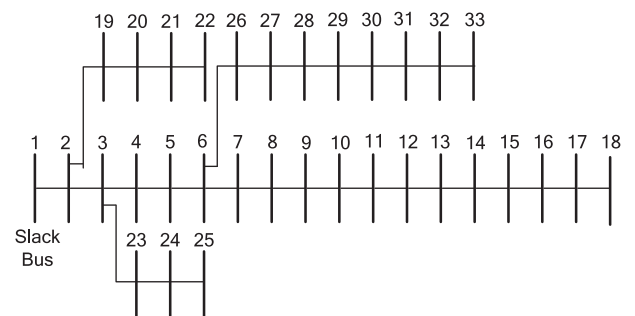


Fig. 6. The IEEE 33-bus radial distribution system.

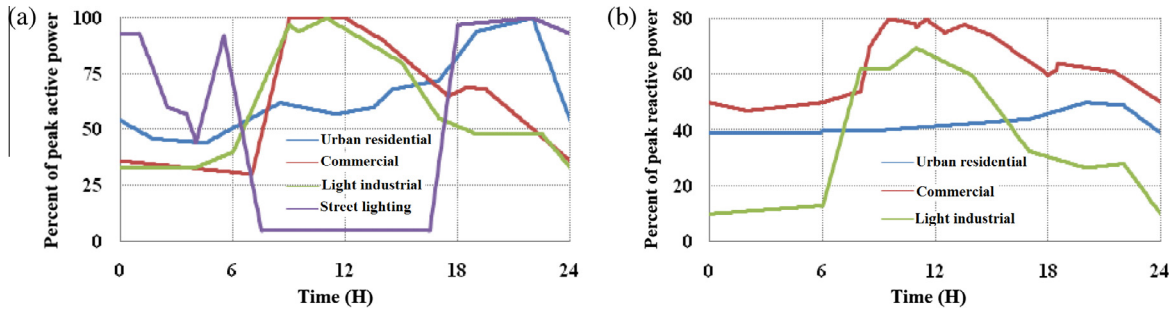


Fig. 7. Daily load curves for the consumer types used in the tests. (a) Active power and (b) reactive power.

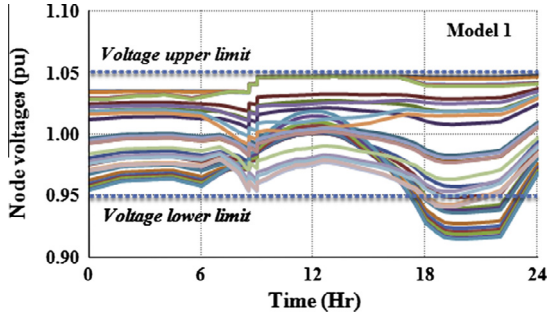


Fig. 8. Voltage profile for all buses during 24 h for Model 1 inverter.

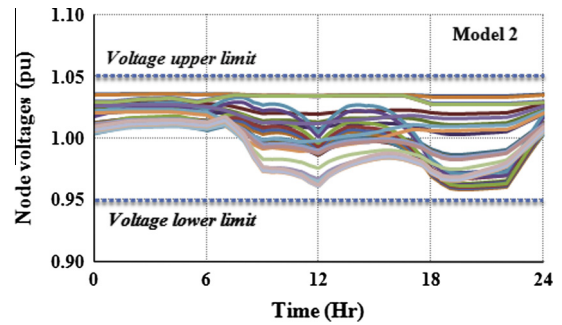


Fig. 10. Voltage profile for all buses during 24 h for Model 2 inverter.

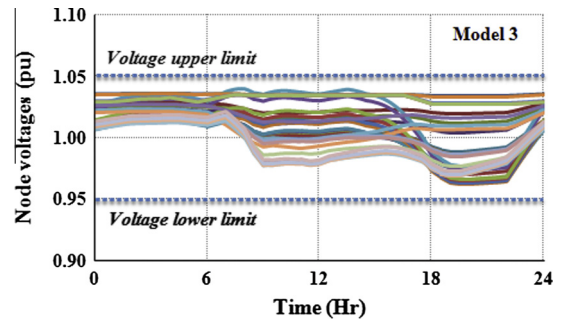


Fig. 11. Voltage profile for all buses during 24 h for Model 3 inverter.

Model 3: The inverter is allowed to generate reactive power for voltage support. The S rating of the inverter is assumed equal to $110\%P_{max}$.

Fig. 8 shows the voltage profile for all buses during 24 h for Model 1 inverter. When the inverter is compliant with IEEE1547, an OLTC is needed to control the voltage within the specified limit. Number of taps required during the 24 h is illustrated in Fig. 9. The resulting voltage profiles show abrupt jumping at the instants of tap changes.

When the PV inverter is designed to generate reactive power for voltage support, the OLTC has not changed as all of the system voltages were within the specified range. This is shown in Figs. 10 and 11 for inverter Models 2 and 3, respectively. The figures show the benefit of allowing the inverter to generate reactive power. Without OLTC, the resulting voltage profiles lie within the desired range without abrupt jump as was the case of Model 1. Figs. 10 and 11 show that the effect of 10% increasing in the PV inverter is greater at the noon time (at full sun), where Model 2 inverter generates no reactive power.

Voltage stability results

Voltage stability results were discussed by calculating and drawing the stable part of the P–V curve of bus 18 up to the SNB

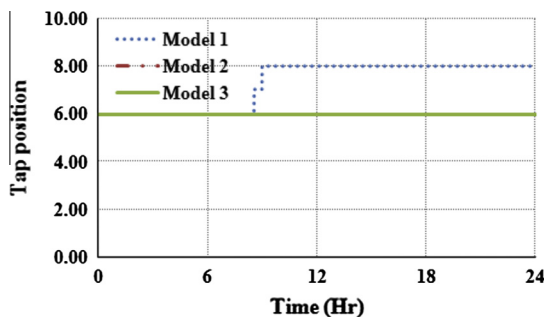


Fig. 9. Taps positions of the three inverter models at the substation transformer.

point. Voltage will collapse if the load is larger than the SNB point. Four different cases were discussed and each case contains the above three models of PV inverter in addition to a fourth scenario at no PV generation. Time period and description of each case are as follows:

- Case 1:** Between 7:00 AM and 7:30 AM with clear sky. This time is chosen during the sun rise in which the insolation increases. All loads are assumed of the light industrial type.
- Case 2:** Between 12:00 PM and 12:30 PM with clear sky. This time is chosen during the maximum insolation. All loads are assumed of the commercial type.
- Case 3:** Between 5:30 PM and 6:00 PM with clear sky. This time is chosen during the sun set in which the insolation decreases to zero. All loads are assumed of the urban residential type.
- Case 4:** Between 12:00 PM and 12:30 PM with cloud sky. This time is chosen during the maximum insolation. PV generation is assumed slowing to 15% per minute up to 20% of its value at this time of the day. All loads are assumed of the commercial type.

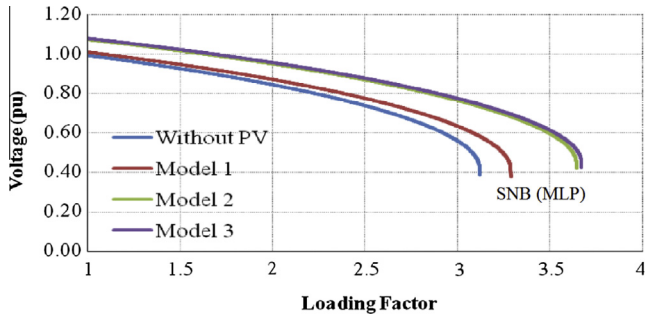


Fig. 12. P–V curves of bus 18 for Case 1: between 7:00 AM and 7:30 AM with clear sky.

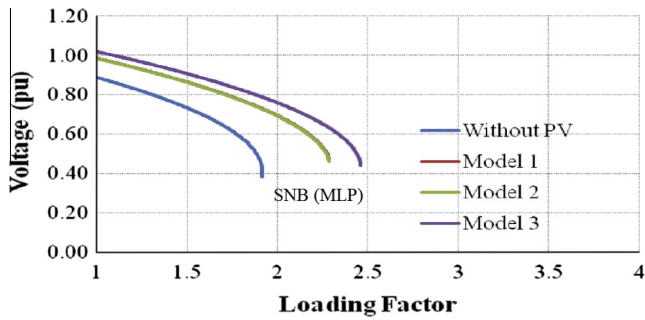


Fig. 13. P–V curves of bus 18 for Case 2: Between 12:00 PM and 12:30 PM with clear sky.

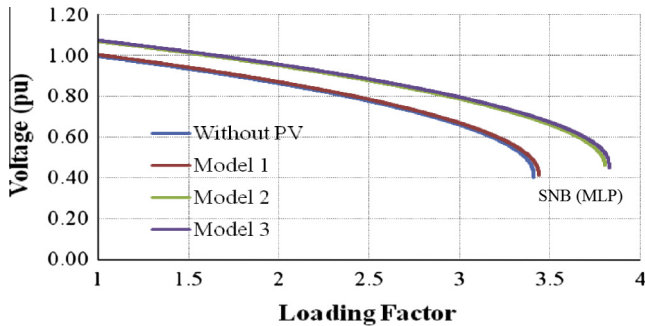


Fig. 14. P–V curves of bus 18 for Case 3: Between 5:30 PM and 6:00 PM with clear sky.

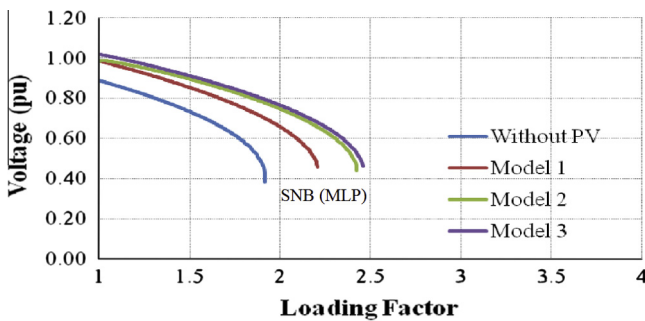


Fig. 15. P–V curves of bus 18 for Case 4: Between 12:00 PM and 12:30 PM with cloud sky.

P–V curves of bus 18 for the above four cases are shown in Figs. 12–15. It is shown in the figures that both real power and reactive power of PV help in enhancing the voltage stability of

Table 2
MLP for cases 1–4.

Cases	Time	Sky	Without PV	PV inverter participation		
				Model 1	Model 2	Model 3
1	7:00–7:30 AM	Clear	3.12	3.28	3.62	3.64
2	12:00–12:30 PM	Clear	1.92	2.28	2.29	2.44
3	5:30–6:00 PM	Clear	3.41	3.44	3.79	3.82
4	12:00–12:30 PM	Clear	1.92	2.20	2.40	2.43

the distribution systems. However, the real power effect is confined only during the noon time at clear sky. During the sun rise, sun rest and cloud sky the effect of real power of PV is limited. This result and the additional knowledge of no sun during evening, entails the necessity of reactive power generation of PV inverter to support voltage and enhance the voltage stability. Fig. 13 shows that the effect of 10% increasing in the PV inverter is greater at the noon time (at full sun) and clear sky. This result in addition to the extra cost of greater inverter rating leads the designer to choose Model 2 for PV inverter. Table 2 summarizes the MLP for the above study cases. The table shows that the benefit of increasing the rating of PV inverter by 10% is little, except for Case 2 (at full sun).

Conclusion

The paper has presented a study of the voltage stability problem in distribution systems with high penetration PV generations which are equipped with reactive power support capabilities. A series of case studies was conducted with different operation modes of the power conditioning unit and at different environment conditions. The calculated results show that reactive power support can positively contribute to feeder voltage regulation and an improved voltage profile. The resulting voltage profiles lie within the desired range without abrupt jump with demand variations. The voltage stability assessment at different scenarios exhibits higher maximum loading condition with reactive power support in comparison with unity power factor operation of the power conditioning unit. The operation of the study system can be further improved by increasing the inverter rating above the maximum real power capacity of the PV module. In this case, the power conditioning unit offers reactive power support in case availability of maximum power for PV module. The effect of a 10% increase in the capacity of the power conditioning unit benefits the system during peak PV generation, noon time with clear sky, by providing reactive power support to support the operation of the system within the desired voltage limit. However, the 10% increase in the inverter size is slightly affects maximum loading conditions of the study system.

Acknowledgment

The first and second authors gratefully acknowledge the contribution of the USA-Egypt Joint Science and Technology Fund for providing partial research funding under the project number STDF-839.

References

- [1] Whitaker C, Newmiller J, Ropp M, Norris B. Distributed photovoltaic systems design and technology requirements. Tech rep. Sandia/SAND2008-0946 P; 2008.
- [2] Villalva Marcelo Gradella, Gazoli Jonas Rafael, Filho Ernesto Ruppert. Comprehensive approach to modeling and simulation of photovoltaic arrays. IEEE Trans Power Electron 2009;24(5):1198–208.
- [3] Tan Yun Tiam, Kirschen Daniel S, Jenkins Nicholas. A model of PV generation suitable for stability analysis. IEEE Trans Energy Convers 2004;19(4):748–55.

- [4] Liu E, Bebic J. Distribution system voltage performance analysis for high-penetration photovoltaics. Tech Rep. NREL/SR-581-42298; 2008.
- [5] Achilles S, Schramm S, Bebic J. Transmission system performance analysis for high-penetration photovoltaics. Tech rep. NREL/SR-581-42300; 2008.
- [6] McGranaghan M, Ortmeyer T, Crudele D, Key T, Smith, Baker J. Advanced grid planning and operation. Tech rep. NREL/SR-581-42294; 2008.
- [7] Yazdani A, Dash PP. A control methodology and characterization of dynamics for a photovoltaic (PV) system interfaced with a distribution network. *IEEE Trans Power Deliv* 2009;24(3):1538–51.
- [8] Tan YT, Kirschen DS. Impact on the power system of a large penetration of photovoltaic generation. *IEEE Power Energy Soc General Meet* 2007:1–8.
- [9] Xue Yaosuo, Manjrekar Madhav, Lin Chenxi, Tamayo Maria, Jiang John N. Voltage stability and sensitivity analysis of grid-connected photovoltaic systems. *IEEE Power Energy Soc General Meet* 2011:1–7.
- [10] Li F, Kueck J, Rizey T, King T. A preliminary analysis of the economics of using distributed energy as a source of reactive power supply. Oak Ridge National Laboratory First Quarterly Report for Fiscal Year; 2006.
- [11] US-Canada Power System Outage Task Force. Final report on the August 14, 2003, Blackout in the United States and Canada: causes and recommendations, at 18th April, 2004.
- [12] Amjady N, Esmaili M. Application of new sensitivity analysis framework for voltage contingency ranking. *IEEE Trans Power Syst* 2005;20(2):973–83.
- [13] Xu Yan, Tom Rizy D, Li Fangxing, Kueck John D. Dynamic voltage regulation using distributed energy resources. In: 19th International conference on electricity distribution (CIRED) Vienna, 21–24 May 2007. Paper 0736.
- [14] Senjyu Tomonobo, Miyazato Yoshitaka, Yona Atsushi, Urasaki Naomitsu, Funabashi Toshihisa. Optimal distribution voltage control and coordination with distributed generation. *IEEE Trans Power Deliv* 2008;23(2):1236–42.
- [15] Oshiro Masato, Tanaka Kenichi, Senjyu Tomonobo, Toma Shohei, Yona Atsushi, Saber Ahmed Yousuf, et al. Optimal voltage control in distribution systems using PV generators. *Elsevier Electr Power Energy Syst* 2011;33:485–92.
- [16] Tanaka Kenichi, Oshiro Masato, Toma Shohei, Yona Atsushi, Senjyu Tomonobo, Funabashi Toshihisa, et al. Decentralized control of voltage in distribution systems by distributed generators. *IET Gener Transm Distrib* 2010;4:1251–60.
- [17] Yun Tiam T, Kirschen DS. Impact on the power system of a large penetration of photovoltaic generation. In: *Proc IEEE power eng soc general meeting*; 2007. p. 1–8.
- [18] Yan Rui Feng, Saha Tapan Kumar. Investigation of voltage stability for residential customers due to high photovoltaic penetrations. *IEEE Trans Power Syst* 2012;27(2):651–62.
- [19] Augugliaro A, Dusonchet L, Mangione S. Voltage collapse proximity indicators for radial distribution networks. In: 9th Int conf on elect power quality and utilization. Barcelona; 9–11, 2007.
- [20] Abdel-Akher M, Bedawy A, Aly MM. Application of bifurcation analysis on active unbalanced distribution system. In: *IET renewable power gen conf, RPG* 2011. Edinburgh, UK; 5–8 September 2011.
- [21] Zhou Y, Ajarapu V. A fast algorithm for identification and tracing of voltage and oscillatory stability margin boundaries. *Proc IEEE* 2005;93(5):934–46.
- [22] IEC 60038 standard. <<http://www.electricalengineering-book.com/voltagesystems.html>>.
- [23] IEEE 1547 standard for interconnecting distributed resources with electric power systems. <<http://grouper.ieee.org/groups/scc21/1547/1547index.html>>.
- [24] Gonzalez Sigifredo, Stein Joshua, Fresquez Armando, Ropp Michael, Schutz Dustin. Performance of utility interconnected photovoltaic inverters operating beyond typical modes of operation. In: 39th IEEE photovoltaic specialists conference, 16–21 June 2013. Tampa, Florida, USA.
- [25] Aly Mohamed, Abdel-Akher Mamdouh. A continuation power-flow for distribution systems voltage stability analysis. In: *IEEE international power and energy conference (PECON 2012)*, 2–5 December 2012. Kota Kinabalu, Malaysia.
- [26] Abdel-Akher Mamdouh. Voltage stability analysis of unbalanced distribution systems using backward/forward sweep load-flow analysis method with secant predictor. *IET Gener Transm Distrib* 2013:19.
- [27] Chapra Steven C, Canale Raymond P. *Numerical methods for engineers*. 5th ed. McGraw Hill; 2006.
- [28] Abdel-Akher M, Mahmoud K. Unbalanced distribution power-flow model and analysis of wind turbine generating systems. *Euro Trans Electr Power* 2013;23(5):689–700.
- [29] Dilek M, de Leon F, Broadwater R, Lee S. A robust multiphase power flow for general distribution networks. *IEEE Trans Power Syst* 2010;25(2):760–7687.
- [30] Xiao Weidong, Dunford William G, Capel Antoine. A novel modeling method for photovoltaic cells. In: *Power electronics specialists conference, (PESC 04)*, IEEE 35th annual, vol. 3; 2004. p. 1950–6.
- [31] Alsayid Basim, Jallad Jafar. Modeling and simulation of photovoltaic cells/modules/arrays. *Int J Res Rev Comput Sci (IJRRCS)* 2011;2(6):1327–31.
- [32] Masters Gilbert M. *Renewable and efficient electric power systems*. A John Wiley & Sons, Inc, Publication; 2004.
- [33] De Soto W, Klein SA, Beckman WA. Improvement and validation of a model for photovoltaic array performance. *Solar Energy* 2006;80:78–88.
- [34] Shell SM50-H Photovoltaic Solar Module. <<http://www.ecomaipo.cl/solar/documentos/shell-SM50-H.pdf>>.
- [35] Yi-Bo Wang, Chun-Sheng Wu, Hua Liao, Hong-Hua Xu. Steady-state model and power flow analysis of grid-connected photovoltaic power system. In: *IEEE international conference on industrial technology, (ICIT 2008)*; 2008. p. 1–6.
- [36] Venkatesh B, Ranjan R, Gooi HB. Optimal reconfiguration of radial distribution systems to maximize loadability. *IEEE Trans Power Syst* 2004;19:260–6.
- [37] Taleski Rubin, Rajicic Dragoslav. Energy summation method for energy loss computation in radial distribution networks. *IEEE Trans Power Syst* 1996;11(2):1104–11.